DYNAMIC LOADS OF CONTROL SYSTEM ELEMENTS

Tamás Gausz*, Zsanna Gausz*
***Deprtment of Aircraft and Ships, Budapest University of Technology and Economics**

Keywords: *control loadings, rotor blade, dynamics*

Abstract

The aim of this article is to give an advisable engineering method applicable to the calculation forces and moments arriving from the rotor side and arisen from the aerodynamic and dynamic effects over the rotor blades. Aerodynamic forces and moments can be estimated by the using of the integrated blade and impulse theory while the unsteady effects and compressibility of the flow can be considered in the blade element theory.

1 Introduction

Forces and moments on the control surfaces or on the rotor blades cause loads appearing on the different parts of the control system. They give the ultimate and the fatigue loads on the concerned control system elements, furthermore the required power and the other parameters of the occurrent additional hydraulic or electrical system are affected by them.

The aim of this article is how to investigate the control forces and moments from the rotor side determined by the rotor blade aerodynamics and dynamics. Aerodynamic forces and moments can be estimated traditionally by the integrated blade element and impulse theory (BEMT). Blade element theory is in which the unsteady effects computed by the using of the shed vortices and the compressibility can be taken into account as well.

The investigation referred to an articulated rotor head includes the rigid flapping, lagging and feathering of the rotor blade. In the operation process the elastic deformations of the rotor blades should be also considered.

The units of this complex rotor model are conventional, but the load estimation requires a lot of unsteady and steady flight regime investigations. Method reviewed in this article can be recommended for such a computations because of its relatively small time demands and acceptable accuracy.

2 Mechanical Model of the Rotor

For the most helicopter rotors the rotor blades are usually connected through the hinges or quasi-hinges to the rotor hub. So that the rotor blades have possibility for flapping, lagging, feathering motions and elastic deformation. This rigid and elastic motions can superpose.

2.1 Rigid Blade Model

The motion of the rigid blades can be described by the applying blade-fixed non-inertial coordinate system. The basic equation of this motion:

$$\boldsymbol{\Theta}\frac{\delta\boldsymbol{\omega}}{\delta t}+\boldsymbol{\omega}\times(\boldsymbol{\Theta}\boldsymbol{\omega})=\mathbf{M}_0-(\boldsymbol{\rho}_s\times\mathbf{a}_0)m \qquad (1)$$

where $\boldsymbol{\Theta}$ – the inertial tensor;

$\frac{\delta\boldsymbol{\omega}}{\delta t}$ – the angular acceleration;

$\mathbf{M}_0$ – the resulting external moments acting to the blade;

$\boldsymbol{\rho}_s$ – the blade center of mass;

$\mathbf{a}_0$ – the acceleration of the origin;

m – the rotor blade mass.

Equation (1) is a vector-differential equation, in general it can be solved numerically. That is why the each element of this equation is generated by the computer. In the elements calculation the conventional coordinate transformations can be successfully used. For instance the angular acceleration is:

$$\frac{\delta \boldsymbol{\omega}}{\delta t} = \dot{\mathbf{A}}_{lr} \left(\mathbf{A}_{rb} \boldsymbol{\omega}_b \right) + \dot{\mathbf{A}}_{lr} \boldsymbol{\Omega}_{MR} + \dot{\boldsymbol{\omega}}_l \tag{2}$$

where $\mathbf{A}_{lr}$ - the transformation between the rotating and blade systems;
$\dot{\mathbf{A}}_{lr}$ - the time derivate of this matrix;
$\boldsymbol{\omega}_b$ - the helicopter angular velocity;
$\boldsymbol{\Omega}_{MR}$ - the main rotor angular velocity;
$\dot{\boldsymbol{\omega}}_l$ - the angular acceleration of the rotor blade.

2.2 Elastic Blade Model

The flapwise bending deformation is an important form of the rotor blade motions. This type of motion can be investigated by the using of normal modes. In the calculation the first normal mode describes the rigid blade motion, the second and third normal modes are used to determine the real elastic deformation.

The latest normal modes should be estimated by the method of "assumed modes". For the bending deflections calculation the next two modal equations can be written as:

$$\varphi_i'' + \lambda^2 \varphi_i = \frac{Q_i}{\Omega^2 R^2 m_i}; \qquad i = 2, 3 \tag{3}$$

where φ_i - the i[th] generalised coordinate;
$\lambda_i \Omega$ - the i[th] natural frequency;
$Q_i = \int_0^L p_b(x)\, S_i(x)\, dx$;
p_b - the external load along the rotor blade.

The local deformation velocity is a part of the perpendicular velocity component (V_z) and has influence to the local angle of attack. The modal equation (3) should be integrated together with the basic differential equation (1).

The complete set of the equations involves the aerodynamic model as well. In the developed model the rigid rotor blades have four degrees of freedom; namely they are the flapping and the lagging motions and two elastic deformations. Since the flapwise torsion is treated as a mechanical constrained motion, it gives the possibility to determinate the blade torsional moment.

3 Aerodynamic Model

The aerodynamic model is based on the BEMT theory and combined with the effect of the shed vortices. The calculation can be executed in the local wind fixed coordinate system. That is why in the calculations we can use the lift, drag and the moment coefficients and we don't need the normal and tangential force coefficients. The resultant air flow velocity at a blade section has three components: V_x, V_y, V_z. The local angle of attack and the resultant velocity in *y-z* plane (V_{res}) should be calculated by the using of the tangential (V_y) and perpendicular (V_z) velocity components. The local sweep angle of the flow is determined by the length velocity component (V_x) and the resultant velocity (V_{res}). The section lift, drag and the moment coefficients for the steady state are functions of the effective angle of attack, the local sweep angle and Mach number:

$$\begin{aligned} c_l &= c_l(\alpha_e, \Lambda, M); \\ c_d &= c_d(\alpha_e, M); \\ c_m &= c_m(\alpha_e, M); \end{aligned} \tag{4}$$

where α_e – the effective angle of attack;
Λ – the local sweep angle;
M – the local Mach number.

3.1 Investigation of the unsteady effects

The unsteady component of the lift and moment coefficients can be treated into inertial and circulatory part.

The inertial part is estimated by the well known method of coupled masses, there the circulatory part is determined by the shed vortices:

$$\Gamma_{si}(t_j) = \frac{c}{2}\left[V_i c_{li}(t_{j-1}) - V_i c_{li}(t_j) \right] \tag{5}$$

where $\Gamma_{si}\left(t_j\right)$ - the shed vortex intensity at the i^{th} place and the j^{th} time, and $j=-1,-2....-n$;

c - the local chord length;

$V_i\, c_{li}\left(t_j\right)$ - the resultant air velocity and the local lift coefficient.

The bound vortex around the blade section element is interpreted at the *0*th time.

As the lift coefficient represents the effect of bound vortex, therefore the circulatory part of the lift can be calculated by the using of the shed vortices.

Applying equation (4) we can get the sequence of the shed vortices remaining the trailing edge of the rotor blades. It opens the way how to calculate the relative position of the shed vortices regard to the rotor blades. Denoting the length of the i^{th} shed vortex by the Δx_{li} and using the Biot-Savart law the induced velocity field of the shed vortices can be found out. Finally to have the induced velocities we can estimate the circulatory part of the lift and moment coefficients.

3.2 Dynamic Stall

As the flow around a rotor blade is generally unsteady it occurs the dynamic stall appearing at a higher angle off attack. The accurate investigation of it is quite difficult task. However at the normal operating range of helicopter rotors the dynamic stall is only partial problem. Because of it we can use quite simple approximation for the determination of the critical angle of attack change:

$$\Delta\alpha_{stall}=\gamma\sqrt{\left|\frac{c\,\dot{\alpha}}{2V_{res}}\right|}\,\mathrm{sgn}\left(\dot{\alpha}\right) \qquad (6)$$

where $\Delta\alpha_{stall}$ – the change of the critical angle of attack;

$\gamma=1.76\ln\left(\frac{0.6}{M}\right)$ – empirical function included the Mach number;

$\dot{\alpha}$ – change in angle of attack for unit time.

Due to the dynamic stall and sweep effect the critical profile angle of attack will change, its value can be or too high or too low. In order to get physically real values we should set bounds on the allowable lift coefficient.

3.3 Rotor blade tip loss calculation

Since the rotor blades are finite wings we should to take into account the tip losses as well. Our new method how to determine the tip-loss factor is

$$c_s(x_l,\psi_r)=\frac{x_l^{q1}\left(L-x_l\right)^{q2}}{\left(\frac{L\,q1}{q1+q2}\right)^{q1}\left(L-\frac{L\,q1}{q1+q2}\right)^{q2}} \qquad (7)$$

where c_s – the tip loss factor;

x_l – the coordinate along the blade;

ψ_r – the blade azimut angle;

L – the blade length;

q_1 *and* q_2 – constants;

$$q2=\frac{c_{lmean}}{1+\frac{1-\cos\left(\psi_r\right)\sin\left(\psi_r\right)}{1+\cos\left(\psi_r\right)\sin\left(\psi_r\right)}}$$

$$q1=K-q2$$

and

$$c_{lmean}=\frac{\sum_{i=1}^{n}\left(c_{li}\,\Delta x_{li}\right)^2}{\sum_{i=1}^{n}\left(\Delta x_{li}\right)^2}$$

c_{li} - lift coefficient of the *i*-th section;

Δx_{li} - length of the *i*-th blade section.

This method takes into account the sweep and the lift coefficient effect to the tip losses.

4 Practical Example

As the results of the numerical model can't be received in closed form solution we have got them in discreet form. To get consequences we have to build up numerical experiment.

To realize the numerical experiment we should develop computer program. The computer code generates the values of the lift, drag and the moment coefficients including the effect of unsteadiness, compressibility and sweep. The actual terms of the equations (1) and (3) are created by this program too. The results of the numerical integration of (1) and (3) are the changing in the flapping and lagging angle, in the bending deformation and in the flapwise torsional moment as a function of the azimut angle.

In this numerical example the rotor diameter is 10.5 meters. The rotor has classical articulated rotor head with flapping, lagging and feathering hinges. The flapping hinge offset is 0.155 meter.

The flapping motion leads to the well known changing in the blade incidence. Therefore we have an aerodynamic damping of the flapping motion. The additional damper damps the lagging motion.

For the numerical presentation of the results the flight velocity is 30 m/s, the angle of attack of the main rotor is –4.3 degrees. In steady horizontal flight the helicopter path angle is zero, therefore the helicopter pitch angle is -4.3 degrees as well.

Collective and cyclic control of the rotor blades can be presented as:

$$p(\psi_r) = p_0 + p_1 \cos(\psi_r - \psi_{r0}) + p_2 \sin(\psi_r - \psi_{r0}) \tag{7}$$

where p_0 - the collective control parameter;

p_1 - the cyclic control parameter refers to the elevator motion;

p_2 - the cyclic control parameter refers to the aileron motion;

ψ_{r0} - control angle due to delay of the rotor blade motions.

4.1 Initial conditions

The rotor model described above does not include the effect of the other helicopter parts (e.g. fuselage, tail boom, horizontal and vertical dampers and tail rotor). This calculation give the results for the steady or quasi steady cases. It means that the magnitude of the flight velocity and the angular velocity components of the fuselage are constants.

The initial conditions of the rotor blade motions are unknown so we should assume that at the beginning the flapping angle and flapping velocity, the lagging angle and lagging velocity the elastic deflections and elastic deformation velocities are equal to zero.

So we can state that the rotor blades should do some rotations to reach its path. In this practical example it does about 10 to 20 rotations. The angular velocity of the main shaft is 38.1 [1/s], this number of rotations takes some seconds. This relatively short period provides us to assume that during this time the flight is steady or quasi steady.

4.2 Generalised equilibrium of rotor blades

Because of the initial conditions described above, the rotor blades move asymptotically to their generalised equilibrium, so that it can be stated that they have a Poincare-stability.

Figure 1. shows the generalised equilibrium state of the rotor blade flapping motion. Well seen that the set of curves is a limited chaotic attractor. It means that the flapping motion of the rotor blade occurs in a well defined finite region, actually in a narrow one. We can assume, that in practice only one path in the phase plane approximates the motion. Therefore tip path and also tip path plane can be ordered to the rotor blade motion.

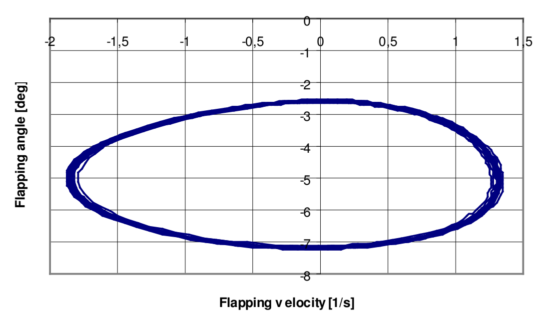

Fig. 1. Phase diagram of the flapping

Of course all the other types of rotor blade motions have a similar generalised equilibrium state.

4.3 Control forces and moments

In this article we show only some typical results such a horizontal flight with constant velocity of

30 m/s, steady turn with the same velocity and bank angle of 30 degrees and nose up manoeuvre with the nose up angular velocity of 0.1 1/s. The numerical model is suitable to take into account the control and the flight parameters.

Using the flapwise torsional moment the force acting to the control rod can be calculated. Figure 2. shows the mean value of the torsional moment in horizontal flight as a function of the azimut angle.

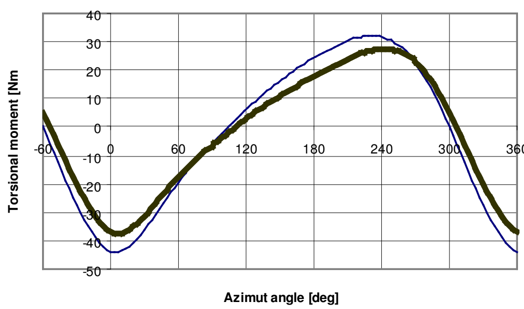

Fig. 2. Control moment

There the thin line presents the control moment acting to the rigid blade and the thick line demonstrates the behaviour of the elastic blade. Because of the limited chaotic attractor of the blade motion the control moment has also chaotic attractor. The figure shows only the mean value of control moment as a function of the azimut angle.

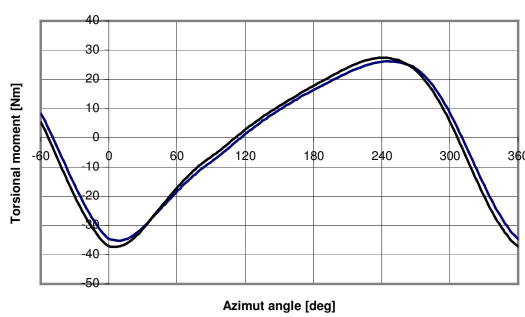

Fig. 3. Control moment in turn

In Figure 3. beside thick line taken out from Figure 2. we present the control moment requires to the left turn. The results show that the difference between this two curves is quite small and have a good congruence with the measurements and practical experience.

Control moments in horizontal flight and in nose up manoeuvre are presented in Figure 4. The difference between these two curves is small again.

The force acting to the control rod can be determined by a simple dividing because the change in the blade pitch angle is moderate. The rod force is demonstrated in Figure 5. In this phase diagram the rod force varies with the flapping angular velocity.

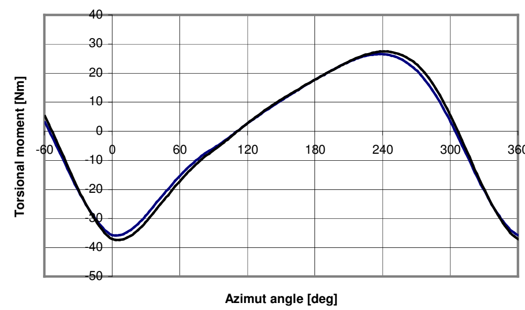

Fig. 4. Control moment in nose up manoeuvre

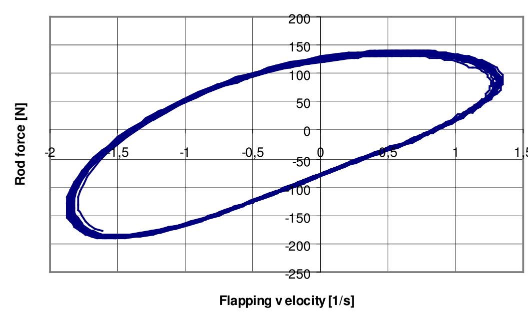

Fig. 5. Phase diagram of the rod force

In this case the equilibrium state is similar to shown in Figure 1. Well seen when the flapping velocity is small the variation in the rod force is also small and it is about 5 – 10 Newtons.

But between the lowest and highest blade position, at the maximum flapping velocities – close to the rear and forward blade position – the rod force variation is notably higher.

The frequency in the variation of the rod force is relatively low.

5 Conclusions

The results of the work reviewed in this article show that in general the control forces and moments are arisen from the rotor side while the normal manoeuvres have no significant effect to them.

Complete investigation and result analyzing prove that the rotor blades motion, forces and moments on them can be characterized by a limited chaotic attractor and only low frequency change was expired.

References

[1] Scanlan, R. H, Rosenbaum, R**.** *Aircraft Vibration and Flutter*. 1st printing, The Macmillen Company, 1951.

[2] Bramwell, A. R. S. *Helicopter Dynamics.* Edward Arnold. Ltd. 1976.

[3] Leishman, J. G. *Principles of Helicopter Aerodynamics.* Cambridge Univ. Press. 2000.

[4] Newman, S. *The Foundations of Helicopter Flight.* Butterworth-Heinemann. 1994.

[5] Dat, R. *Development of Basic Methods needed to Predict Helicopter Aeroelastic Behaviour.* Vertica, Vol.8. No. 2. pp. 209-228, 1984.

[6] Bergh, H. Wekken, A. J. P. *Comparison between Measured and Calculated Stall-Flutter Behaviour of aOne-Bladed Model Rotor.* Vertica, Vol. 11. No.3. pp.447-456. 1987.

[7] Gausz, T. *Aerodynamic and Dynamical Investigation of Helicopter Rotors.* ICAS Conference 2000. ICA0182

[8] Prouty, R. W. *Helicopter Performance, Stability and Control.* Krieger Publ. Company 1986.